UCRL-17651 Rev.
cy. 2

University of California

Ernest O. Lawrence Radiation Laboratory

RARE DECAY MODES OF $N^*(1950)$

W. Chinowsky, P. Condon, R. R. Kinsey, S. Klein, M. Mandelkern, P. Schmidt, J. Schultz, F. Martin, M. L. Perl, and T. H. Tan

March 1968

TWO-WEEK LOAN COPY

This is a Library Circulating Copy which may be borrowed for two weeks. For a personal retention copy, call Tech. Info. Division, Ext. 5545

UCRL - 17651 Rev. cy. 2

DISCLAIMER

This document was prepared as an account of work sponsored by the United States Government. While this document is believed to contain correct information, neither the United States Government nor any agency thereof, nor the Regents of the University of California, nor any of their employees, makes any warranty, express or implied, or assumes any legal responsibility for the accuracy, completeness, or usefulness of any information, apparatus, product, or process disclosed, or represents that its use would not infringe privately owned rights. Reference herein to any specific commercial product, process, or service by its trade name, trademark, manufacturer, or otherwise, does not necessarily constitute or imply its endorsement, recommendation, or favoring by the United States Government or any agency thereof, or the Regents of the University of California. The views and opinions of authors expressed herein do not necessarily state or reflect those of the United States Government or any agency thereof or the Regents of the University of California.

Submitted to Physical Review

UCRL-17651 Rev.
Preprint

UNIVERSITY OF CALIFORNIA
Lawrence Radiation Laboratory
Berkeley, California

AEC Contract No. W-7405-eng-48

RARE DECAY MODES OF $N^*(1950)$

W. Chinowsky, P. Condon, R. R. Kinsey, S. Klein, M. Mandelkern,
P. Schmidt, J. Schultz, F. Martin, M. L. Perl, and T. H. Tan

March 1968

RARE DECAY MODES OF N*(1950) *

W. Chinowsky, P. Condon,+ R. R. Kinsey,++ S. Klein, M. Mandelkern,+
P. Schmidt, and J. Schultz+

Physics Department and Lawrence Radiation Laboratory,
University of California, Berkeley, California

and

F. Martin, M. L. Perl, and T. H. Tan

Stanford Linear Accelerator Center, Stanford, California

ABSTRACT

An analysis of p-p interactions at 6 BeV/c indicates the presence of a T=3/2 nucleon resonance with mass near 2.0 BeV/c^2, with decay modes $Y^{*+}(1385)K^+$, $N^{*++}(1236)\rho^0$, and $N^{*++}(1236)\pi^+\pi^-$. A peripheral production model for the reaction $pp \rightarrow nN^{*++}(1950)$ gives excellent agreement with the data, with a cross section for $N^{*++}(1950)$ production and subsequent decay into $Y^{*+}K^+$ of 13 ± 3 μb.

---

* Work performed under the auspices of the U. S. Atomic Energy Commission.

+ Present address: University of California, Irvine.

++ Present address: Brookhaven National Laboratory, Upton, New York

Subject category 63.6

I. INTRODUCTION

Proton-proton inelastic reactions have been demonstrated often to be dominated by production of nucleon isobars, particularly the $N^*(1236)$.[1-19] Higher mass nucleon isobars are also produced copiously. Analyses, particularly of production angular distributions, show that the reactions are peripheral and probably dominated by pion exchange processes. Detailed study of multi-particle final states indicates that many of their features may be understood to result from quasi-two-body production reactions.[10-19] Thus, three-particle final states are produced most often from $pp \to N^{*++} + n$, $N^{*+} + p$, and four-particle final states from $pp \to N^{*++} + N^{*0}$, $N^{*+} + p$. Five-body states, because of experimental difficulties, have not been as precisely delineated. These are of particular interest because they allow a determination of partial widths for nucleon resonance decay into many particles. In the present paper we present evidence for the production of an I=3/2 nucleon isobar of mass near 2.0 BeV/c^2 in the reaction $pp \to N^{*++}n$, with decay modes $N^{*++} \to N^{*++}(1236)\rho^0$ where $N^{*++}(1236) \to p\pi^+$ and $\rho^0 \to \pi^+\pi^-$, and $N^{*++} \to Y^{*+}(1385)K^+$ where $Y^{*+}(1385) \to \Lambda\pi^+$.

II. DATA

With a proton beam having a transport momentum of 6.04 ± 0.03 BeV/c and negligible contamination, 550,000 pictures were obtained in the LRL 72-inch liquid hydrogen bubble chamber.[20] In one-fifth of the film, approximately 33,000 non-strange four-prong events were measured on the LRL Flying Spot Digitizer and processed with the reconstruction and kinematic fitting programs FOG-CLOUDY. All the film was scanned for events

with visible charged or neutral decays; these were measured on conventional machines and reconstructed with the PACKAGE program. It is important to note that the data presented here have been obtained with two different measuring and analyzing schemes, so that the consistency in the observed features of the $n\Lambda\pi^+K^+$ and $np\pi^+\pi^+\pi^-$ final states supports the argument that these have not been caused by some fault in the analysis.

a. Non-Strange Particle Events

In the four-prong data, the identified states and their production cross-sections are

(1)	$pp \to pp\ \pi^+\pi^-$	3.2 ± 0.3 mb
(2)	$pp \to pn\pi^+\pi^+\pi^-$	3.1 ± 0.5 mb
(3)	$pp \to pp\ \pi^+\pi^-\pi^0$	2.4 ± 0.4 mb

Reaction (1) is observed to be dominated by peripheral production of pseudo-two-body final states N^*N and N^*N^*. This is consistent with earlier work at other energies,[10,11,14,15,17] as is the lack of ρ-meson production in the four-body state.[10,11,21] Reactions (2) and (3), however, yield particles whose final state interactions are qualitatively different from those of process (1). In particular, analysis of events identified as examples of reaction (2) reveals evidence for ρ meson production, the $\pi^+\pi^-$ mass spectrum showing a peak in excellent agreement with the known ρ-meson properties. In addition, there is an indication of a peak near 2.1 BeV/c^2 in the distribution of $p\pi^+\pi^+\pi^-$ combined mass of all events produced by reaction (2). This effect becomes stronger when $N^{*-}(1236) \to n\pi^-$ production is eliminated by restricting the data to a sample with $n\pi^-$ mass outside the interval 1220 ± 100 MeV/c^2. The background under the $\rho \to \pi^+\pi^-$ peak is also decreased

by this selection. The $p\pi^+\pi^+\pi^-$ mass distribution for 2521 events after this selection is given in the unshaded histogram of Fig. 1. Also drawn for comparison is a phase space curve for 64 percent $np\pi^+\pi^+\pi^-$ and 36 percent $nN^{*++}(1236)\pi^+\pi^-$, the relative rates obtained from analysis of the $p\pi^+$ mass spectrum. This background curve is the mass distribution of events generated by a Monte Carlo method, with the same selection on $n\pi^-$ mass; the normalization has been determined from the events with $M(p\pi^+\pi^+\pi^-) \geq 2.3$ BeV/c^2. Although statistical distributions are of limited significance in these interactions dominated by peripheralism and pseudo-two-body final states, it is useful for illustrating the general shape of the $p\pi^+\pi^+\pi^-$ spectrum, and for demonstrating structure due to dynamical effects. Other backgrounds which include two-body or multi-body decay modes of various nucleon resonances are not significantly different in shape.

The enhancement is observed in the $T_z=3/2$ state, and therefore has isotopic spin T=3/2. A similar peak is seen in the $p\pi^+\pi^-\pi^0$ combined mass of the final state $pp\pi^+\pi^-\pi^0$. However, only the state $np\pi^+\pi^+\pi^-$ will be analyzed in detail here; it is possible to eliminate background events with greater confidence and one also expects that T=3/2 effects will occur with larger production cross-sections in the $p\pi^+\pi^+\pi^-$ state.

Further restrictions on the data are made with the purpose of increasing the signal to background ratio, and of isolating a production reaction and final state that is amenable to comparison with a dynamical model, specifically $pp \rightarrow nN^{*++}(1236)\rho^0$. Thus we next require that at least one of the two possible $p\pi^+$ mass combinations be inside the $N^{*++}(1236)$ mass region 1220 ± 60 MeV/c^2. Of 1492 events, 259 have both effective mass

combinations within these limits. The $p\pi^+\pi^+\pi^-$ and $\pi^+\pi^-$ mass distributions are presented in the middle histogram of Fig. 1 and the unshaded histogram of Fig. 2, respectively. Both mass combinations are plotted when it is not possible to identify only one of the two π^+ as an N^{*++} decay product. The $\pi^+\pi^-$ mass spectrum shows evidence for considerable ρ-meson production, which had previously not been detected in p-p interactions.[10,11,21,22] The inclusion of both $\pi^+\pi^-$ mass combinations for the non-unique events does not affect the height of the ρ peak but only increases the smoothly varying background.

In the spirit of peripheralism, it is then required that $|\cos\theta_n| \geq 0.9$, where θ_n is the angle, in the total center-of-system, between the direction of the neutron and the beam proton. The mass spectra of the remaining 582 events, or 704 combinations, are plotted in the bottom histogram of Fig. 1 and the shaded histogram of Fig. 2. It should be pointed out that although the background has been considerably decreased by all these selections, the number of events in the $p\pi^+\pi^+\pi^-$ peak has changed very little.

Finally, we demand that the $\pi^+\pi^-$ mass be in the ρ region, 740 ± 100 MeV/c^2. Except for five events in a total of 198, this selection uniquely assigns one π^+ to the N^{*++} and the other to the ρ. The corresponding $p\pi^+\pi^+\pi^-$ mass distribution is shown in Fig. 3. A sizable peak near 2.05 BeV/c^2 is clearly present.

Some evidence that these events are produced by resonance decay and not, perhaps, a kinematic enhancement, is provided by the angular distribution of the $N^{*++}(1236)$ in the $N^*\pi\pi$ center of mass. For events in the resonant region, defined as $1960 \leq M(N^*\pi\pi) \leq 2160$ MeV/c^2, this distribution

is consistent with the forward-backward symmetry characteristic of a resonance decay superimposed on a forward-peaked background; the rest of the events have only a forward peak. The histograms are displayed in Figs. 4a and 4b, respectively. The initial proton used to define the reference direction is that which yields the smaller value of four-momentum transfer squared to the $N^*\pi\pi$ system, consistent with the observed peripheral character of the production process.

b. Strange-Particle Events

A similar enhancement is seen at about 2040 MeV/c^2 in the $\Lambda\pi K$ mass spectrum of the reaction $pp \rightarrow N\Lambda\pi K$. The various channels and their reaction cross-sections are

(4)	$pp \rightarrow p\Lambda\pi^+K^0$	67 ± 10 μb
(5)	$pp \rightarrow p\Lambda\pi^0K^+$	45 ± 7 μb
(6)	$pp \rightarrow n\Lambda\pi^+K^+$	50 ± 7 μb

Although the peak occurs in all these reactions, the most profitable for further analysis is (6). The $\Lambda\pi^+K^+$ system has $T_z=3/2$, which is again the best state for the study of the properties of a system with isospin 3/2. In addition, there is no background from $K^*(890)$ and very little from $N^{*+}(1236) \rightarrow n\pi^+$. The subsequent discussion will therefore only be concerned with the $n\Lambda\pi^+K^+$ final state. The $\Lambda\pi^+K^+$ mass distribution for 680 events is given in the unshaded histogram of Fig. 6, along with a background curve drawn for a mixture of 82 percent $n\Lambda\pi^+K^+$ phase space and 18 percent $nY^{*+}(1385)K^+$ phase space. The normalization for this curve and the fraction of Y^* are appropriate to the events with $M(\Lambda\pi^+K^+) > 2.3$ BeV/c^2.

Once again defining $\cos\theta_n$ to be the angle, in the over-all center of mass, of the neutron direction with that of the beam proton, we

select events with $|\cos\theta_n| \geq 0.9$. The consequent $\Lambda\pi^+K^+$ mass spectrum of 225 events is presented in the shaded histogram of Fig. 5; the peak at 2040 MeV/c^2 is now much more distinct.

The $\Lambda\pi^+$ combined mass before, and after, the neutron angle restriction is shown in the unshaded, and shaded, histograms of Fig. 6, respectively. There is considerable production of Y*(1385) and, in particular, very little background under the Y* peak for those events remaining after the selection on neutron angle.

By imposing the additional requirement that the $\Lambda\pi^+$ mass be within the Y*(1385) region, $M(\Lambda\pi^+) = 1385 \pm 35$ MeV/c^2, we obtain a nearly pure sample of $pp \rightarrow nY^{*+}(1385)K^+$. The final $\Lambda\pi^+K^+$ mass plot of 100 events in Fig. 7 indicates that the peak near 2040 MeV/c^2 is a direct consequence of Y* production. The various restrictions have produced a sample with strongly decreased background; the peak has diminished very little.

The angular distributions of the Y* in the Y*K rest frame are presented in Fig. 8 (a) for events with $1960 \leq M(Y^*K) \leq 2160$ MeV/c^2, and in Fig. 8 (b) for events with M(Y*K) outside those limits. It is difficult, with these plots, to form any conclusions about the origin of the peak.

III. INTERPRETATION

Since small momentum transfer to the neutron is favored in both the reaction $pp \rightarrow nY^{*+}K^+$ and $pp \rightarrow nN^{*++}\pi^+\pi^-$, $Y^{*+}K^+$ and $N^{*++}\pi^+\pi^-$ ass distributions consistent with phase space are not to be expected. As is well known, the kinematics of such reactions requires that low values of effective mass be enhanced. To determine whether this effect is sufficient to produce the

observed distributions, we compare the data with the predictions of a peripheral production model as illustrated in Fig. 9. The differential cross section for the final state $nN^*\rho$ is then written

$$\frac{d^2\sigma}{dm^2 d\Delta^2} = \text{const} \times \frac{\Delta^2}{(\Delta^2+m_\pi^2)^2} \frac{P}{m} e^{-\alpha\Delta^2} \tag{1}$$

where Δ^2 = four-momentum transfer squared to the neutron,

m = effective mass of $N^*\rho$,

P = momentum of the ρ or N^* in the $N^*\rho$ center of mass.

This form is chosen to yield agreement with the observed momentum transfer distribution. The factor $\Delta^2/(\Delta^2+m_\pi^2)^2$ is for convenience in later calculations with the explicit one-pion-exchange mechanism as a model for peripheral production.[23] Included in addition is an exponential dependence on momentum transfer $e^{-\alpha\Delta^2}$. We determine the parameter α from the experimental distribution in Δ^2 without, of course, restricting the data to events with $|\cos\theta_n| \geq 0.9$. For the $N^*\pi\pi$ events, a good fit is obtained with $\alpha_{N^*\pi\pi} = 1.0 \pm 0.5\ (\text{BeV/c})^{-2}$, while the $Y^{*+}K^+$ events yield $\alpha_{Y^*K} = 0.5 \pm 0.5\ (\text{BeV/c})^{-2}$.

With $\alpha_{N^*\pi\pi} = 1.0$, events were generated by a Monte Carlo method for $pp \to nN^{*++}\rho^0$ according to Eq. (1), and for $pp \to nN^{*++}\pi^+\pi^-$ with a three-body phase space factor replacing P/m in Eq. (1). The resonance shapes of the mass distributions of $p\pi^+$ from $N^{*++}(1236)$ decay and of $\pi^+\pi^-$ from ρ^0 decay were included, and the events were subjected to the experimental restrictions on $p\pi^+$ and $\pi^+\pi^-$ combined mass and $|\cos\theta_n|$. As can be seen in Fig. 2, there are roughly equal amounts of resonant ρ and non-resonant $\pi^+\pi^-$ within the region $M(\pi^+\pi^-) = 740 \pm 100\ \text{MeV/c}^2$. The Monte

Carlo events were therefore combined in the same proportion. The consequent $N^{*++}\pi^+\pi^-$ "peripheral phase space" distribution is shown as the smooth curve of Fig. 3. The fit to the experimental histogram is poor: $\chi^2=27$ for nine constraints. There is similarly poor agreement with the Δ^2 distribution obtained with events restricted to $|\cos\theta_n| \geq 0.9$. It is concluded that a phase space distribution, modified to give the observed forward-peaked production angular distribution, is not sufficient to explain the $N^{*++}\pi^+\pi^-$ mass spectrum, so that some interaction in the final states $N^{*++}\pi^+\pi^-$ and/or $N^*\rho^0$ is indicated. With $\alpha_{Y^*K}=0.5$, similar conclusions are obtained from comparison of the $Y^{*+}K^+$ mass histogram with the calculated spectrum shown as the smooth curve of Fig. 7. Again the fit is poor: $\chi^2=46$ for seven constraints. The experimental momentum transfer distribution for the restricted sample with $|\cos\theta_n| \geq 0.9$ also does not agree with the calculated. Thus, a $Y^{*+}K^+$ resonant interaction is indicated as well.

A natural interpretation of the $N^{*++}\pi^+\pi^-$ and $Y^{*+}K^+$ peaks is that they represent alternate decay modes of a T=3/2 excited nucleon state. To determine the parameters of this resonance, we use only the $Y^{*+}K^+$ data, with the requirement that those parameters yield calculated $N^{*++}\pi^+\pi^-$ spectra in agreement with the observed. This procedure is necessary because there is rather more background in the $nN^{*++}\pi^+\pi^-$ events, specifically non-resonant $p\pi^+$ and non-resonant $\pi^+\pi^-$ within the $N^{*++}(1236)$ and ρ mass regions.

We will seek to fit the $Y^{*+}K^+$ mass spectrum with a combination of resonance and peripheral phase space where, for the resonant $Y^{*+}K^+$ interaction, the phase space factor p/m in Eq. (1) is replaced by the resonant

dependence on m,

$$\frac{m\Gamma(m)}{(m_o^2-m^2)^2 + m_o^2\,\Gamma_t^2(m)}$$

where m_o = nominal resonance mass,

$\Gamma(m)$ = energy-dependent partial width for decay into Y*K, and

$\Gamma_t(m) = \Gamma_{el}(m) + \Gamma_{in}(m)$ is the energy-dependent total width, the sum of the elastic and total-inelastic widths.

For the energy dependence of the widths, we use a formulation in terms of an empirical parameter b, which is a measure of the inverse of the interaction radius:[24]

$$m\Gamma(m) \sim \frac{p}{m}\left(\frac{p^2}{p^2+b^2}\right)^{\ell}$$

where p = momentum of either decay particle in the resonance center of mass and ℓ = decay angular momentum.

An attempt at a precise determination of all the resonance parameters is certainly doomed because of the surfeit of variables, the lack of a precise formulation of energy-dependent resonance widths, and the small number of events. We will therefore only describe qualitatively the variation of χ^2 in a fit of Monte Carlo generated events to the experimental $Y^{*+}K^+$ mass distribution as we vary the fraction of resonance, the nominal resonance mass m_o, the total width at resonance $\Gamma_t(m_o)$, the decay angular momentum ℓ, and the inverse interaction radius b.

The main decay modes of a resonance must be known so that the proper energy dependence may be put into the total width $\Gamma_t(m)$. It is assumed that the major decay of any hypothesized new resonance is predominantly

inelastic, and that the principal mode is $N^*(1236)\pi$. The exception will be the case of $\ell=3$, where we obtain a reasonable fit using a mass and width consistent with those of $N^*(1950)$ inferred from πp scattering. Since this resonance is known to have an elasticity of about 0.5,[25,26] the energy dependence can be characterized by 50% elastic and 50% inelastic, or $N^*(1236)\pi$, decay. The fraction of resonance required to describe the $Y^{*+}K^+$ mass spectrum is .85 ± .15; the uncertainty represents the range through which the fractional rate for resonance production moves as the other parameters are varied over reasonable values. The best fit, achieved for an s-wave decay hypothesis, yields a mass $m_o = (2035 \pm 20)\text{MeV}/c^2$, a total width $\Gamma_t(m_o) = (200 \pm 50)$ MeV and $\chi^2 = 0.1$ for four constraints. For other decay angular momenta, then, b=0.0 will be favored, since this situation is identical to that of s-wave decay. The best fit mass and width for various fixed values of b and ℓ are summarized in Table I.

It appears that these data can accommodate a large variety of resonances near 2.0 BeV/c^2, with parameters that are rather sensitive to the form factor b. The relatively small number of events and the presence of background in the decay angular distributions prevent a determination of its spin and parity or decay angular momentum. Therefore the question of the existence of a new resonance, rather than identification with an established state, cannot be answered.

IV. N*(1950) DECAY MODES

Although evidence for several new T=3/2 resonances near 2.0 BeV/c^2 has been presented,[25] the only firmly established one remains the N*(1950) in the F_{37} partial wave. The entry in Table I for $\ell=3$ and b=0.20 gives good agreement with the presently known mass and width of the N*(1950).[25,26,27] The dashed curves in Fig. 3 and Fig. 7, representing 100% decay of $N^{*++}(1950)$ into $N^{*++}\rho^0$ and $Y^{*+}K^+$, respectively, were calculated with b=0.20 BeV/c, m_o=1940 MeV/c^2 and $\Gamma_t(m_o)$=190 MeV.[28] Best agreement with the data is obtained with a sum of peripheral phase space and resonance decay: 85±15% resonance in $Y^{*+}K^+$ and 55±15% in $N^{*++}\pi^+\pi^-$. It is therefore reasonable to identify the observed peaks as new decay modes

$$N^{*++}(1950) \rightarrow N^{*++}(1236) + \rho^0(760)$$

$$N^{*++}(1950) \rightarrow N^{*++}(1236) + \pi^+ + \pi^-$$

$$N^{*++}(1950) \rightarrow Y^{*+}(1385) + K^+ \quad .$$

It should be noted that the above analysis rests on the assumption that the Breit-Wigner resonance shape, with this particular formulation of the energy-dependence of the widths in terms of the parameter b, is valid to a good approximation at values of mass more than a half-width distant from m_o.

The cross-section for $pp \rightarrow nN^{*++}(1950)$ and the subsequent decay $N^{*++}(1950) \rightarrow Y^{*+}K^+$ is 13 ± 3 μb; this includes corrections for the experimental limits imposed on neutron angle and Y* mass interval. The cross-sections for $N^{*++}(1950) \rightarrow N^{*++}(1236)\rho^0$ and $N^{*++}(1236)\pi^+\pi^-$ are much more difficult to extract. The $N^{*++}\pi^+\pi^-$ mass spectrum of 198 events after all the selection criteria is a consequence of several possible processes,

viz, $N^{*++}(1236)\pi^+\pi^-$ and $N^{*++}(1236)\rho^0$ final states from $N^{*++}(1950)$ decay, peripheral non-resonant production and other background. The fit to this spectrum yields an uncorrected cross-section for $N^*(1950)$ production of 55 ± 15 μb. The proper corrections and separation into the various processes requires knowledge of the $p\pi^+$ and $\pi^+\pi^-$ mass distributions for each. A plot of the $N^{*++}\pi^+\pi^-$ combined-mass distribution for events with $\pi^+\pi^-$ mass outside the selected ρ mass interval clearly indicates that the decay $N^{*++}(1950) \rightarrow N^{*++}(1236)\pi^+\pi^-$ is present. To determine the cross-section, one needs a model for quasi-three-body decay that includes proper angular momentum barrier dependences. Because of all these difficulties, it is only possible to give an estimate of less than 200 μb and probably about 100 μb for the cross-section of $pp \rightarrow nN^{*++}(1950)$, $N^{*++}(1950) \rightarrow N^{*++}(1236)\rho^0$.

Other decay modes of $N^{*++}(1950)$ produced in $pp \rightarrow nN^{*++}(1950)$ have also been reported: Σ^+K^+ with 22±4 μb,[20] and $p\pi^+$ with 320±160 μb[29] and 520±260 μb.[30] Although the inelastic modes $N^*(1236)\pi$ and $N\rho(760)$ are likely to be quite large, their $T_Z=3/2$ states cannot be identified in pp interactions in a bubble chamber because there are necessarily two unobserved neutral particles. The other isospin projections are of course relatively suppressed and are hence difficult to untangle from all the other final states.

One may make various consistency tests and predictions with these cross sections using information from πp phase shift analysis and the requirements of SU_3 invariance. The former finds an elasticity $X(m_0)$ of about 0.5 so that, at resonance, the sum of all the inelastic widths should approximately equal the elastic width. With $N^*(1950)$ as a Regge recurrence of $N^*(1236)$, it is assigned to a decuplet and one finds the following ratios of couplings for $N^{*++}(1950)$ decay:

$$G^2_{\Sigma^+K^+} = G^2_{p\pi^+}$$

$$G^2_{(N^*\pi)^{++}} = 2.5\ G^2_{Y^{*+}K^+} \quad .$$

With our model for the process $pp \to nN^*(1950)$, these yield the cross-section relations

$$\sigma(np\pi^+) = 2.5\ \sigma(n\Sigma^+K^+)$$

$$\sigma(nN^{*++}\pi^0 + nN^{*+}\pi^+) = 13.2\ \sigma(nY^{*+}K^+) \quad .$$

The measured cross sections are $\sigma(np\pi^+) = 375\pm135\ \mu b$, a weighted average of the two values given above, $\sigma(n\Sigma^+K^+) = 22\pm4\ \mu b$ and $\sigma(nY^{*+}K^+) = 13\pm3\ \mu b$. Thus strict SU_3 invariance leads to the prediction

$$\sigma(nN^{*++}\pi^0 + nN^{*+}\pi^+) = 170\pm40\ \mu b\ ;$$

as expected, $N^*(1950) \to N^*(1236) + \pi$ is a major inelastic decay mode. Within our model for $N^*(1950)$ formation in pp interactions we find that

$$\frac{\Gamma_{N^*\pi}(m_o)}{\Gamma_{\pi p}(m_o)} \approx \frac{\sigma(nN^{*++}\pi^0+nN^{*+}\pi^+)}{\sigma(np\pi^+)} \approx 0.4\pm0.2 \quad .$$

These partial widths have not been measured directly. However, the measured elasticity of the resonance provides a relation between the sum of the inelastic widths and $\Gamma_{\pi p}(m_o)$, or

$$\frac{\Gamma_{N^*\pi}(m_o)+\Gamma_{N\rho}(m_o)+\Gamma_{n\pi\pi}(m_o)+\Gamma_{\Sigma K}(m_o)+ \text{----}}{\Gamma_{\pi p}(m_o)} = \frac{X(m_o)}{1-X(m_o)} \approx 1.0\pm0.3 \quad ,$$

where the stated uncertainty is a measure of the differences in the elasticity quoted by authors of different analyses of πp scattering.[25,26] With the reasonable assumption that the partial widths of the decay modes $N^*(1950) \to p\rho^+$, $(N^*(1236)\pi)^{++}$ and $(N\pi\pi)^{++}$ are comparable in magnitude,

one may still accomodate other sizable partial widths and find that, within the rather large uncertainties, SU_3 requirements are satisfied for the $Y^{*+}K^+$ and $(N^*\pi)^{++}$ modes. On the other hand, the measured ratio $\sigma(n\Sigma^{+}K^{+})/\sigma(np\pi^{+})$ appears to disagree with strict SU_3 invariance. The ratio of the cross sections $\sigma(np\pi^{+})$ and $\sigma(nN^*\pi)$ is also conistent with the assumption that

$$m\Gamma(m) = k\,\frac{p}{m}\left(\frac{p^2}{p^2 + b^2}\right)^{\ell}$$

with the same constant k for $p\pi$ and $N^*\pi$ decay. This coupling leads to the prediction that $\sigma(N^{*++}\rho^{o}) \approx 30\ \mu b$ and $\sigma(p\rho^{+}) \approx 120\ \mu b$.[31]

There has been a report of a much more narrow enhancement at 2080 MeV/c^2 in $N^*(1236)\rho$ in a final state produced by $\pi^- p$ collisions.[34] It is unclear whether this peak, observed in the T_z=1/2 state, is related to the phenomena discussed here.

ACKNOWLEDGMENTS

We gratefully acknowledge the cooperation of Professor Luis Alvarez in making the bubble chamber available and Professor Emilio Segrè's much appreciated advice and support. We also wish to thank Professor J. D. Jackson for many fruitful discussions. Dedicated performance of the operating crews of the Bevatron and bubble chamber, as well as the scanners and data analysis personnel, were essential to the performance of the experiment and we thank them all.

REFERENCES

1. K. J. Foley, R. S. Jones, S. J. Lindenbaum, W. A. Love, S. Ozaki, E. D. Platner, C. A. Quarles, and E. H. Willen, Phys. Rev. Letters 19, 397 (1967).

2. I. M. Blair, A. E. Taylor, W. S. Chapman, P. I. P. Kalmus, J. Litt, M. C. Miller, D. B. Scott, H. J. Sherman, A. Astbury, and T. J. Walker, Phys. Rev. Letters 17, 789 (1966).

3. E. W. Anderson, E. J. Bleser, G. B. Collins, T. Fujii, J. Menes, F. Turkot, R. A. Carrigan, Jr., R. M. Edelstein, N. C. Hien, T. J. McMahon, and I. Nadelhaft, Phys. Rev. Letters 16, 855 (1966).

4. C. M. Ankenbrandt, A. R. Clyde, B. Cork, D. Keefe, L. T. Kerth, W. M. Layson, and W. A. Wenzel, Nuovo Cimento 35, 1052 (1965).

5. G. Cocconi, E. Lillethun, J. P. Scanlon, C. A. Stahlbrandt, C. C. Ting, J. Walters, and A. M. Wetherell, Phys. Letters 8, 134 (1964).

6. D. V. Bugg, A. J. Oxley, J. A. Zoll, J. G. Rushbrooke, V. E. Barnes, J. B. Kinson, W. P. Dodd, G. A. Doran, and L. Riddiford, Phys. Rev. 133, B1017 (1964).

7. G. G. Chadwick, G. B. Collins, P. J. Duke, T. Fujii, N. C. Hien, M. A. R. Kemp, and F. Turkot, Phys. Rev. 128, 1823 (1962).

8. G. Cocconi, A. N. Diddens, E. Lillethun, G. Manning, A. E. Taylor, T. G. Walker, and A. M. Wetherell, Phys. Rev. Letters 7, 450 (1961).

9. G. B. Chadwick, G. B. Collins, C. E. Swartz, A. Roberts, S. DeBenedetti, N. C. Hien, and P. J. Duke, Phys. Rev. Letters 4, 611 (1960).

10. A. P. Colleraine and U. Nauenberg, Phys. Rev. 161, 1387 (1967).

11. G. Alexander, O. Benary, G. Czapek, B. Haber, N. Kidron, B. Reuter,

A. Shapira, E. Simopoulou, and G. Yekutieli, Phys. Rev. 154, 1284 (1967).

12. S. Coletti, J. Kidd, L. Mandelli, V. Pelosi, S. Ratti, V. Russo, L. Tallone, E. Zampieri, C. Caso, F. Conte, M. Dameri, C. Grosso, and G. Tomasini, Nuovo Cimento 49A, 479 (1967).

13. A. M. Eisner, E. L. Hart, R. I. Louttit, and T. W. Morris, Phys. Rev. 138, B670 (1965).

14. G. Alexander, O. Benary, B. Haber, N. Kidron, A. Shapira, G. Yekutieli, and E. Gotsman, Nuovo Cimento 40A, 839 (1965).

15. E. L. Hart, R. I. Louttit, D. Luers, T. W. Morris, W. J. Willis, S. S. Yamamoto, Phys. Rev. 126, 747 (1962).

16. W. J. Fickinger, E. Pickup, D. K. Robinson, and E. O. Salant, Phys. Rev. 125, 2082 (1962).

17. E. Pickup, D. K. Robinson, and E. O. Salant, Phys. Rev. 125, 2091 (1962).

18. G. A. Smith, H. Courant, E. C. Fowler, H. Kraybill, J. Sandweiss, and H. Taft, Phys. Rev. 123, 2160 (1961).

19. Robert Ronald Kinsey, "Zero Strangeness Resonance Production in 6 GeV/c Proton-Proton Collisions", (Ph.D. Thesis), University of California Lawrence Radiation Laboratory Report UCRL-17707, March 1968.

20. W. Chinowsky, R. R. Kinsey, S. L. Klein, M. Mandelkern, J. Schultz, F. Martin, M. L. Perl, and T. H. Tan, UCRL-17619; to be published in Phys. Rev. Jan. 25, 1968.

21. E. L. Hart, R. I. Louttit, and T. W. Morris, Phys. Rev. Letters 9, 133 (1962).

22. H. L. Anderson, S. Fukui, D. Kessler, K. A. Klare, M. V. Sherbrook, H. J. Evans, R. L. Martin, E. P. Hincks, N. K. Sherman, P. I. P. Kalmus, Phys. Rev. Letters 18, 89 (1967).

23. A one-pion exchange model has been applied to the reactions $pp \rightarrow N\Lambda\pi K$ and yields fine agreement with the experimental distributions.

24. S. L. Glashow and A. H. Rosenfeld, Phys. Rev. Letters 10, 192 (1963).

25. A. Donnachie, R. G. Kirsopp, and C. Lovelace, Phys. Letters 26B, 161 (1968).

26. P. Bareyre, C. Bricman, and G. Villet, Phys. Rev. 165, 1730 (1968).

27. A. H. Rosenfeld, N. Barash-Schmidt, A. Barbaro-Galtieri, L. R. Price, M. Roos, P. Söding, W. J. Willis, and C. G. Wohl, UCRL-8030 Rev., and to be published in Rev. Mod. Phys. (1968).

28. An interaction radius 1/b of 1 fermi corresponds to b=0.20 BeV/c. With b=0.25±.01 BeV/c, excellent agreement with a variety of data has been obtained by G. Wolf, Phys. Rev. Letters 19, 925 (1967).

29. See Ref. 11. The quoted error is from the fitting procedure only.

30. This cross section is a preliminary value based on our current analysis of the $np\pi^+$ final state in 6 BeV/c pp interactions.

31. Another angular momentum barrier function, adapted from J. M. Blatt and V. F. Weisskopf, Theoretical Nuclear Physics (John Wiley and Sons, New York, 1952), is often used in the analysis of resonances (See refs. 32 and 33). This energy dependence, for decay angular momentum $\ell=3$, as applied in our model with an interaction radius of 1 fermi, leads to cross sections approximately half as large relative to $pp \rightarrow nN^{*++}(1950)$, $N^{*++}(1950) \rightarrow p\pi^+$ as the Glashow-Rosenfeld function. The predicted cross section $\sigma(N^{*++}\rho^0)$ is then about 40 μb. Also, for $\ell=3$ and to about 10% accuracy, the Blatt-Weisskopf function with 1.8 fermi yields the same results as the Glashow-Rosenfeld function with 1.0 fermi.

32. R. D. Tripp, D. W. G. Leith, A. Minten, R. Armenteros, M. Ferro-Luzzi, R. Levi-Setti, H. Filthuth, V. Hepp, E. Kluge, H. Schneider, R. Barloutaud, P. Granet, J. Meyer, and J. P. Porte, Nuclear Physics B3, 10 (1967).

33. W. Layson, Nuovo Cimento 27, 724 (1963).

34. T. S. Yoon, P. Berenzi, A. W. Key, J. D. Prentice, N. R. Steenberg, and W. D. Walker, Physics Letters 24B, 307 (1967).

FIGURE CAPTIONS

Fig. 1. The $p\pi^+\pi^+\pi^-$ mass spectrum of the final state $np\pi^+\pi^+\pi^-$ as various selection criteria are imposed sequentially. These are, in turn: $M(n\pi^-)$ is outside the $N^*(1236)$ mass region (2521 events), $M(p\pi^+)$ is inside the $N^*(1236)$ mass region (1492 events, 1751 combinations) and the cosine of the production angle of the neutron is greater than 0.9 (582 events, 704 combinations).

Fig. 2. The $\pi^+\pi^-$ mass spectrum of the final state $np\pi^+\pi^+\pi^-$. The unshaded histogram represents events with $M(m\pi^-)$ outside and $M(p\pi^+)$ inside the $N^*(1236)$ mass region (1492 events, 1751 combinations). The events in the shaded histogram have the additional restriction that the cosine of the production angle of the neutron is greater than 0.9 (582 events, 704 combinations).

Fig. 3. The $p\pi^+\pi^+\pi^-$ mass spectrum with all the selection criteria as in Fig. 1, as well as the requirement that $M(\pi^+\pi^-)$ be in the ρ mass region (193 events).

Fig. 4. Angular distributions of N^{*++} in the $N^{*++}\pi^+\pi^-$ center of mass for events (a) in the resonant region and (b) outside the resonant region.

Fig. 5. The $\Lambda\pi^+K^+$ mass distribution of the final state $n\Lambda\pi^+K^+$. The unshaded histogram is a plot of the total sample of 680 events; the shaded histogram corresponds to the requirement that the cosine of the production angle of the neutron be greater than 0.9 (225 events).

Fig. 6. The $\Lambda\pi^+$ mass distribution of the final state $n\Lambda\pi^+K^+$. The unshaded histogram displays events for which the cosine of the production

angle of the neutron is greater than 0.9 (225 events).

Fig. 7. The $\Lambda\pi^+K^+$ mass spectrum with all the selection criteria as in Fig. 6, as well as the requirement that $M(\Lambda\pi^+)$ be in the Y^* mass region (100 events).

Fig. 8. The angular distributions of the Y^* in the Y^*K center of mass (a) in the resonant region and (b) outside the resonant region.

Fig. 9. Exchange mechanisms favored by the experimental selections for the processes (a) $pp \rightarrow nN^{*++}\rho^0$ and (b) $pp \rightarrow nY^{*+}K^+$.

Table I. Results of fit to $Y^{*+}K^{+}$ mass spectrum .

Decay Angular Momentum ℓ	b	Resonance Mass m_o	Total Width $\Gamma_t(m_o)$	χ^2 for 4 Constraints
0		2035 ± 20	200 ± 50	0.1
1	.20	2010 ± 25	240 ± 70	1.1
	.35	1990 ± 25	230 ± 70	2.1
2	.20	1980 ± 35	230 ± 70	2.1
	.35	1930 ± 35	200 ± 70	3.7
3	.20	1940 ± 55	190 ± 45	3.1
	.35	1850 ± 55	70 ± 45	7.9

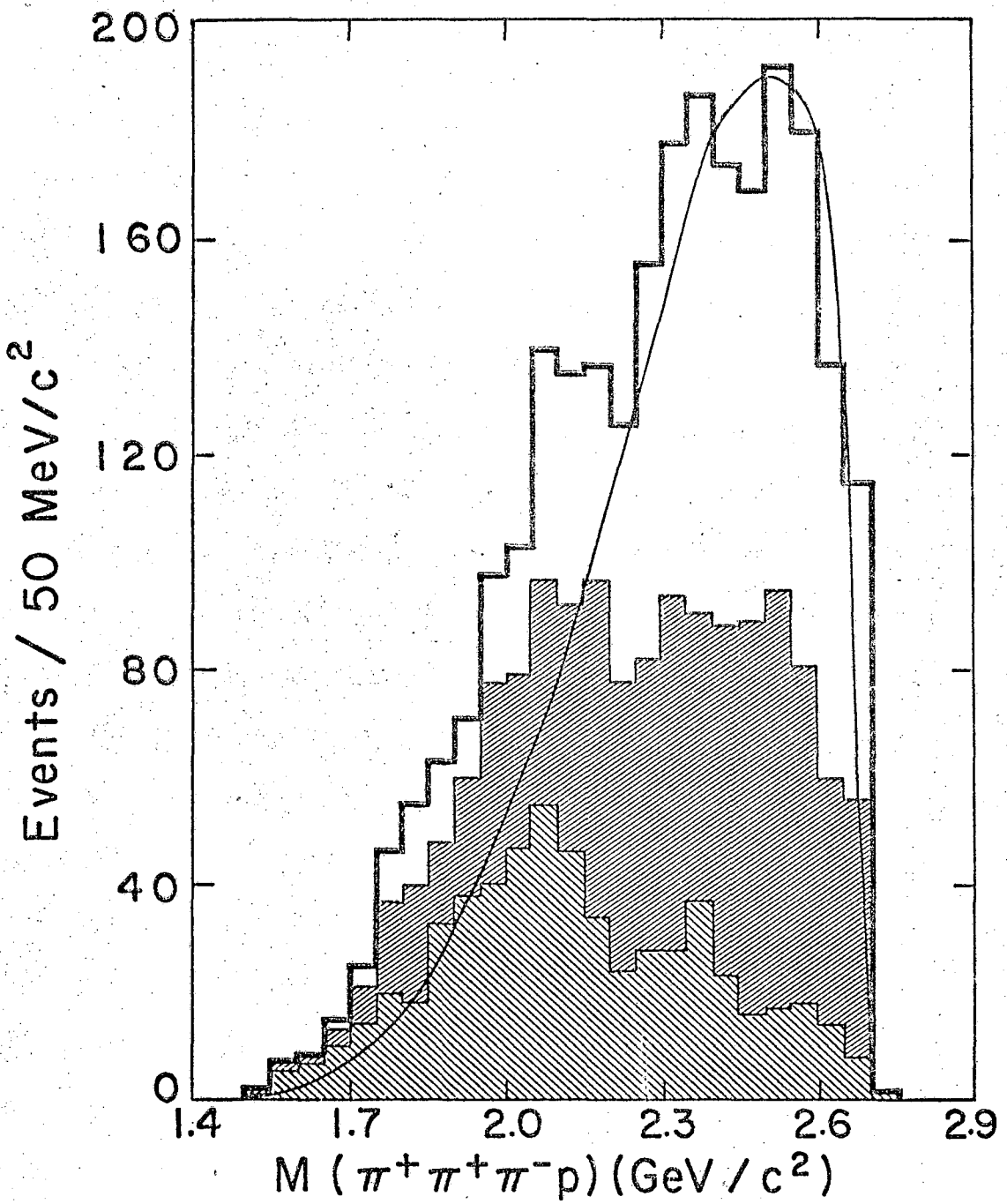

XBL6712-5986

Fig. 1

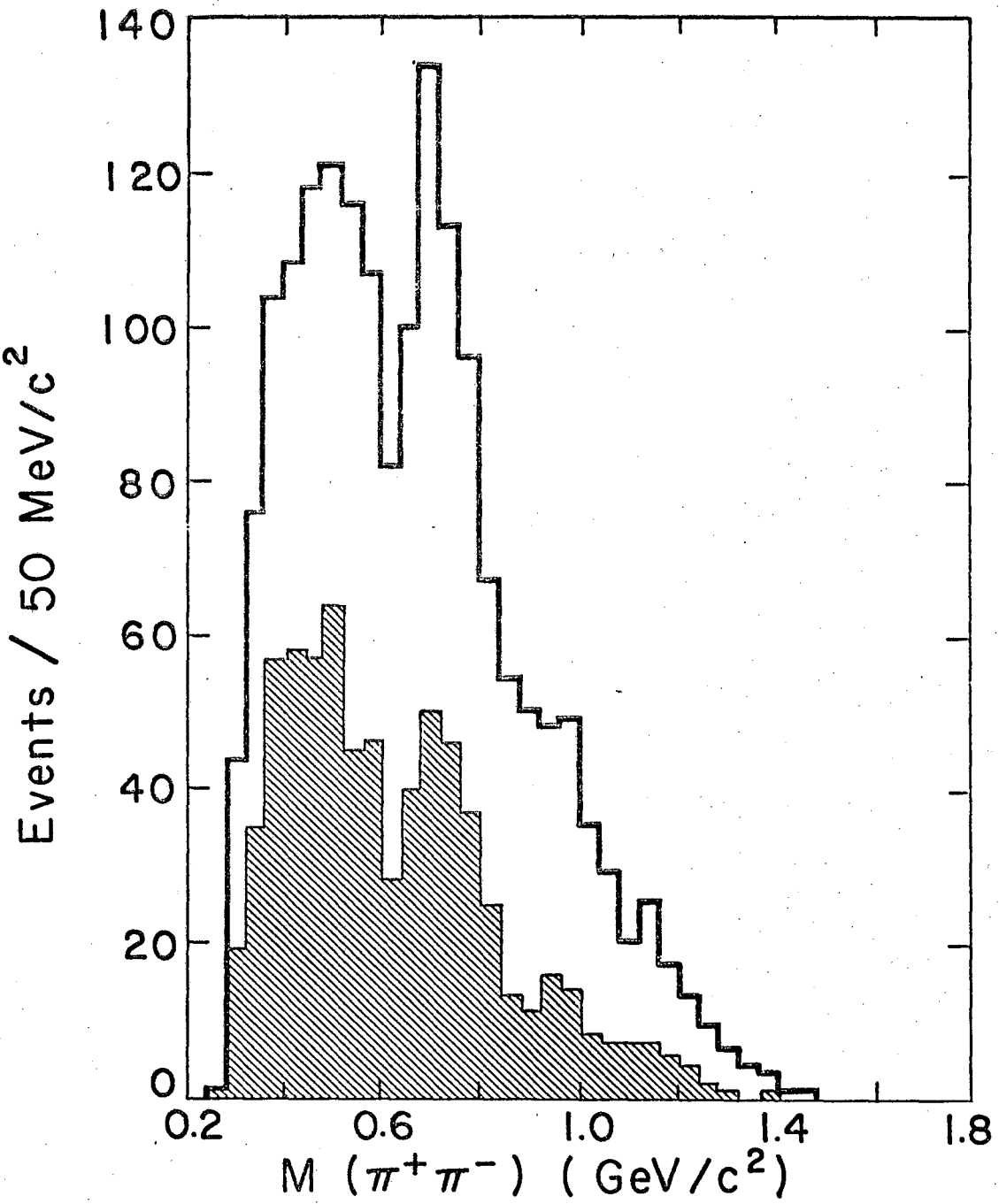

XBL6712-5985

Fig. 2

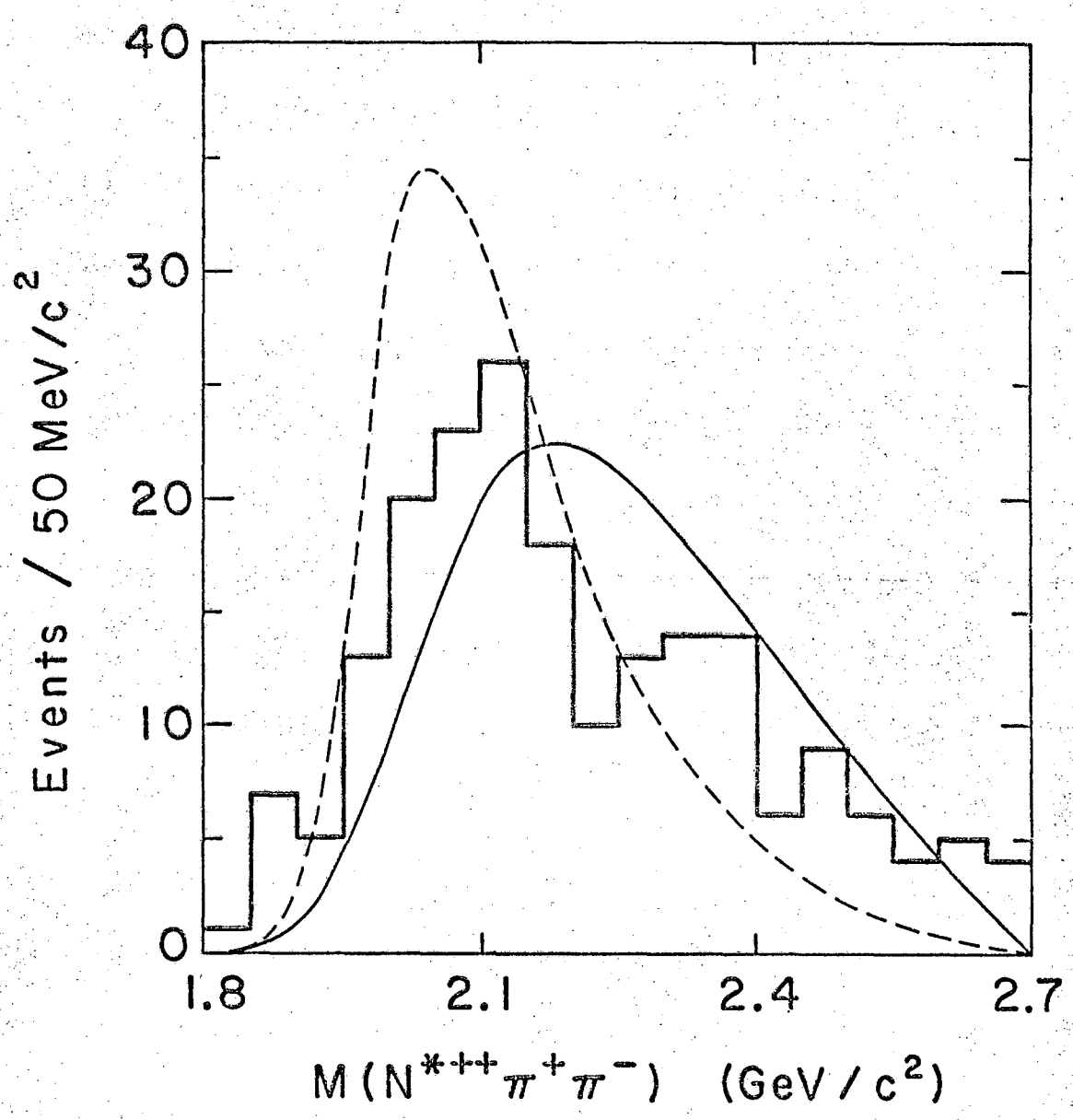

XBL6712-5940

Fig. 3

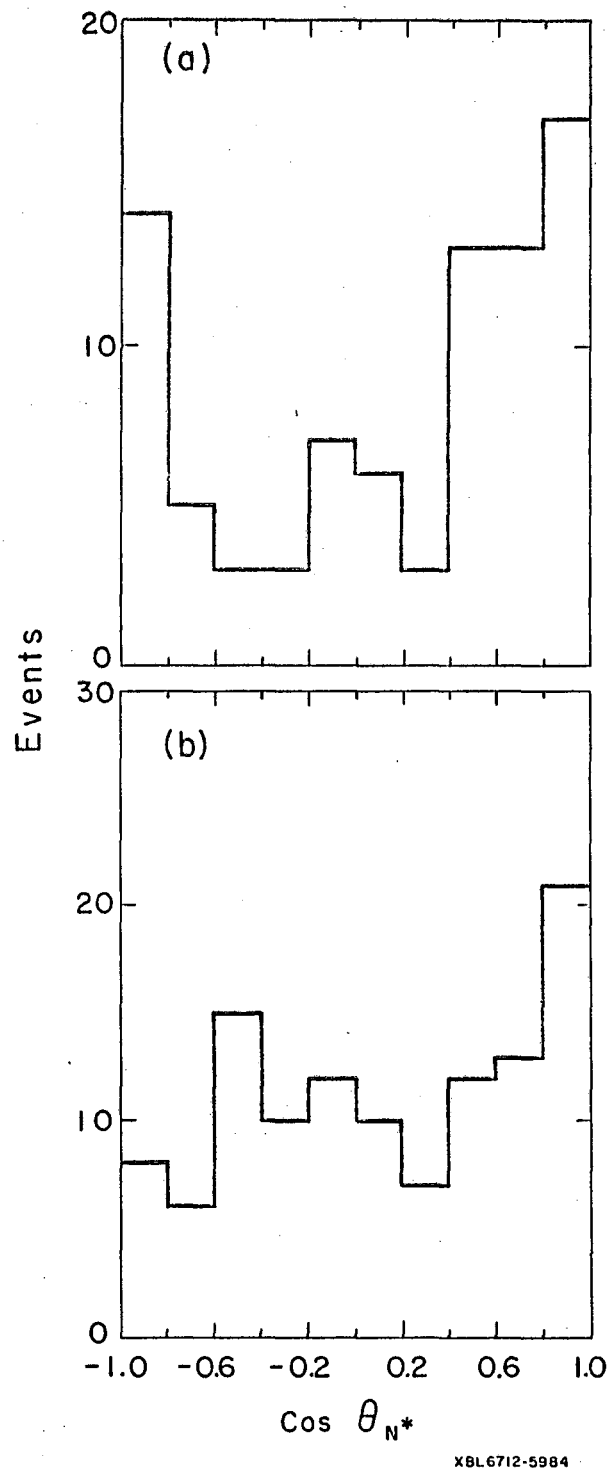
20
(a)
10
0
Events
30
(b)
20
10
0
-1.0
-0.6
-0.2
0.2
0.6
1.0
Cos θ_{N^*}
XBL6712-5984

Fig. 4

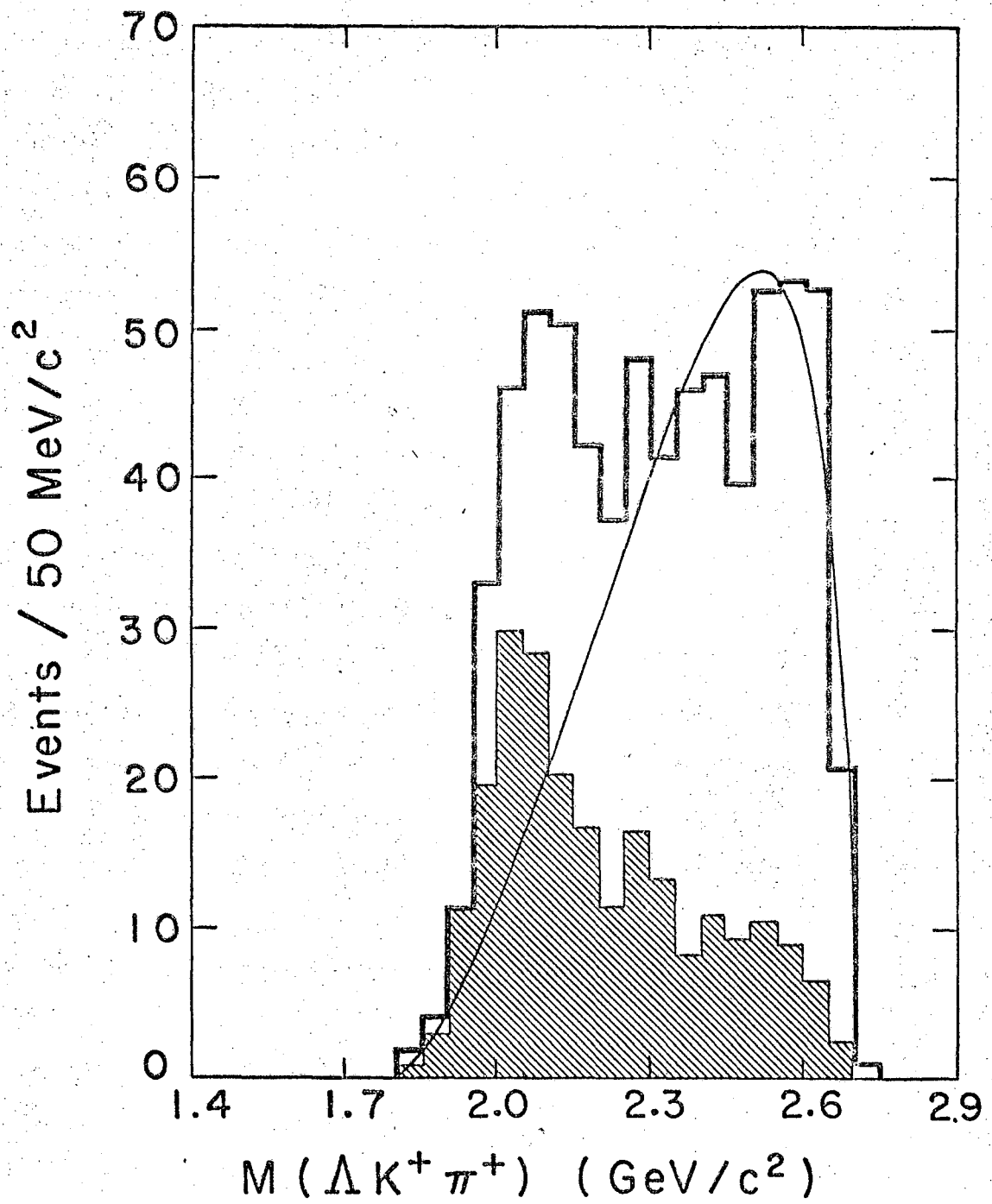

XBL6712-5987

Fig. 5

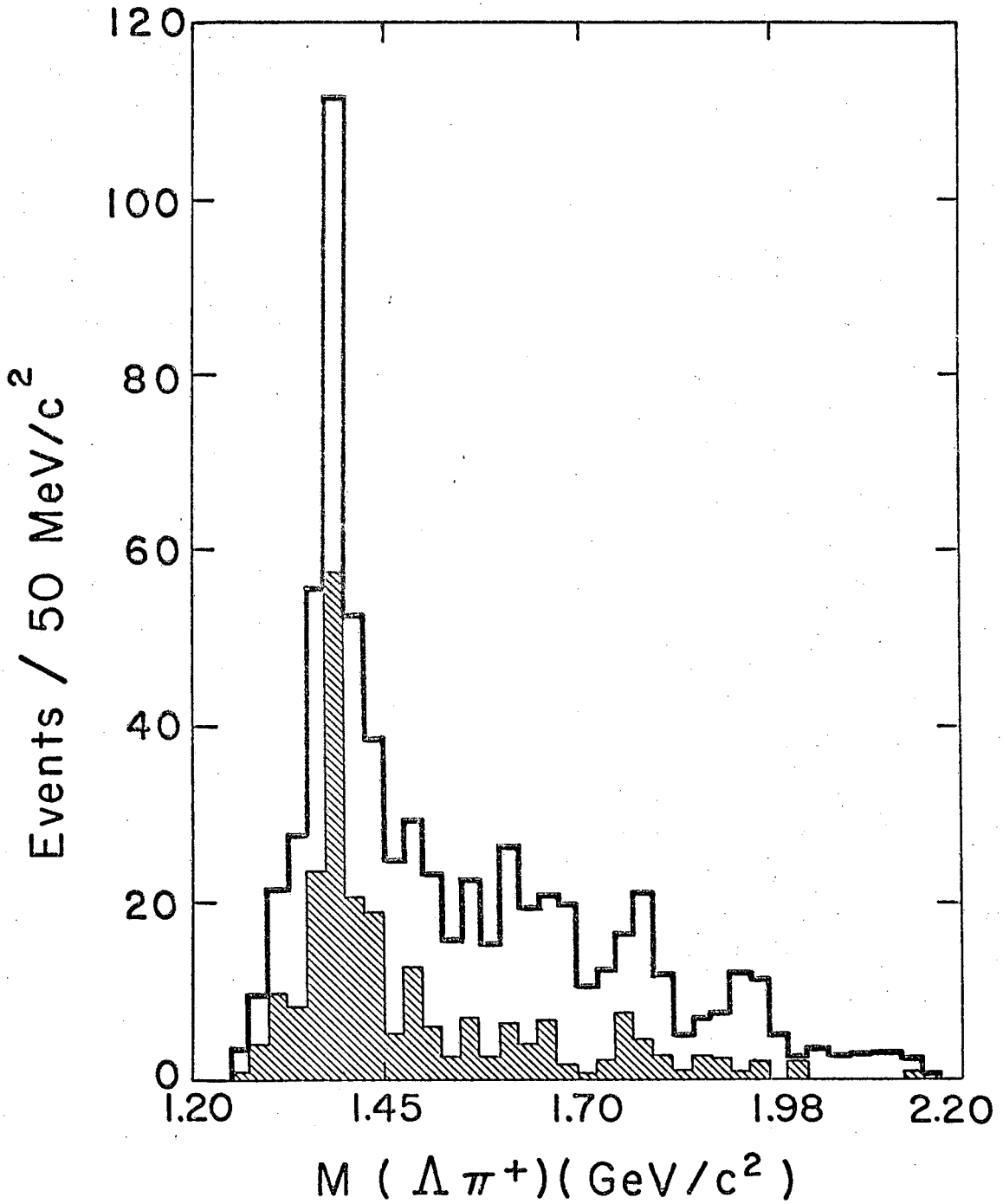

XBL678-3781-A

Fig. 6

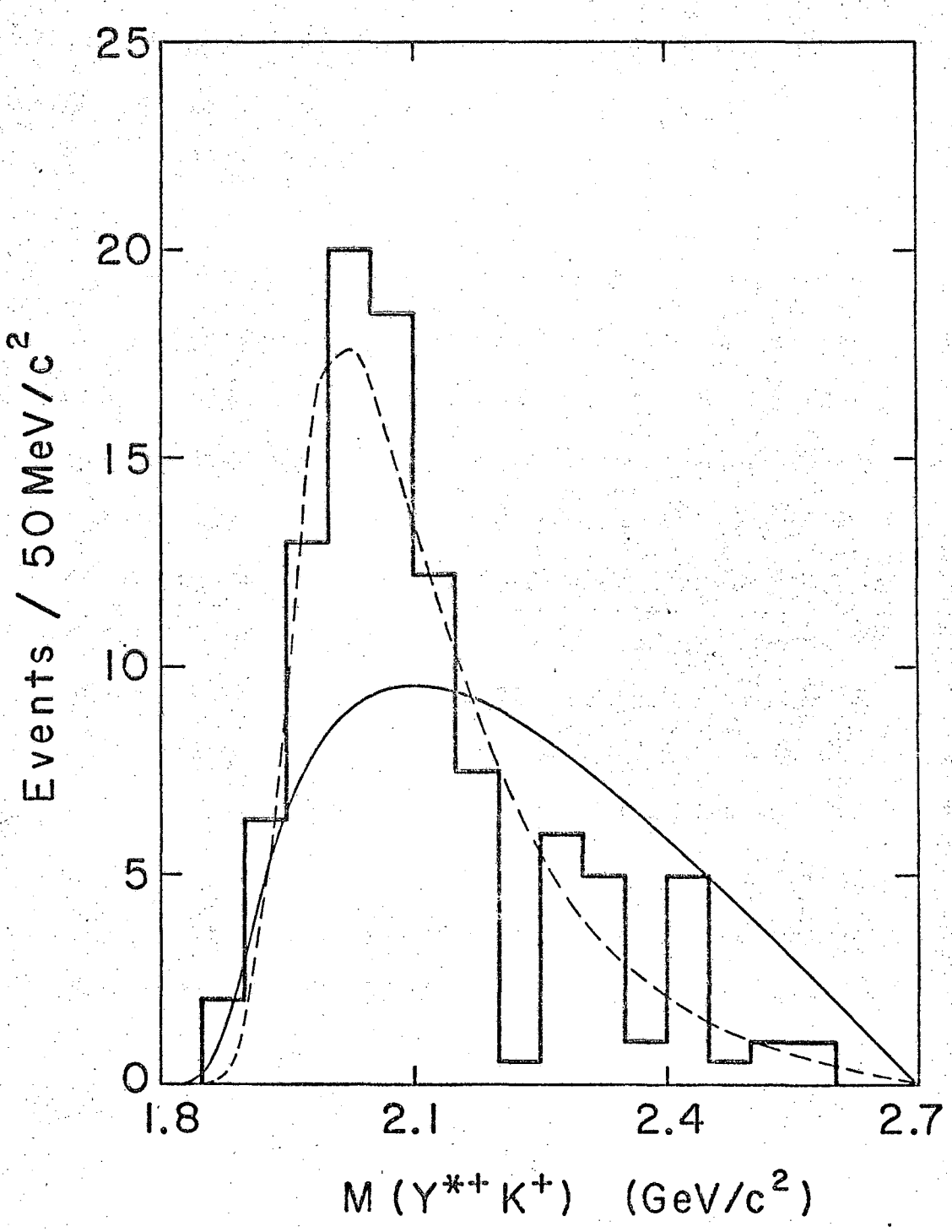

XBL6712-5939

Fig. 7

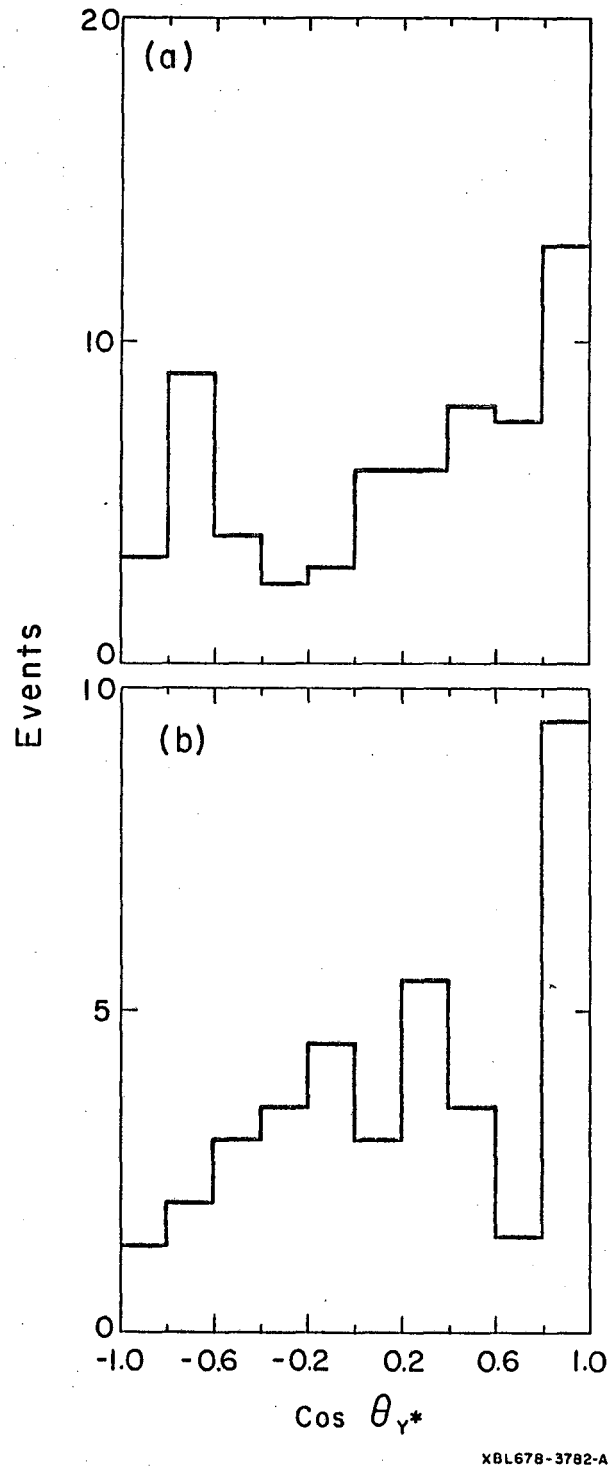

Fig. 8

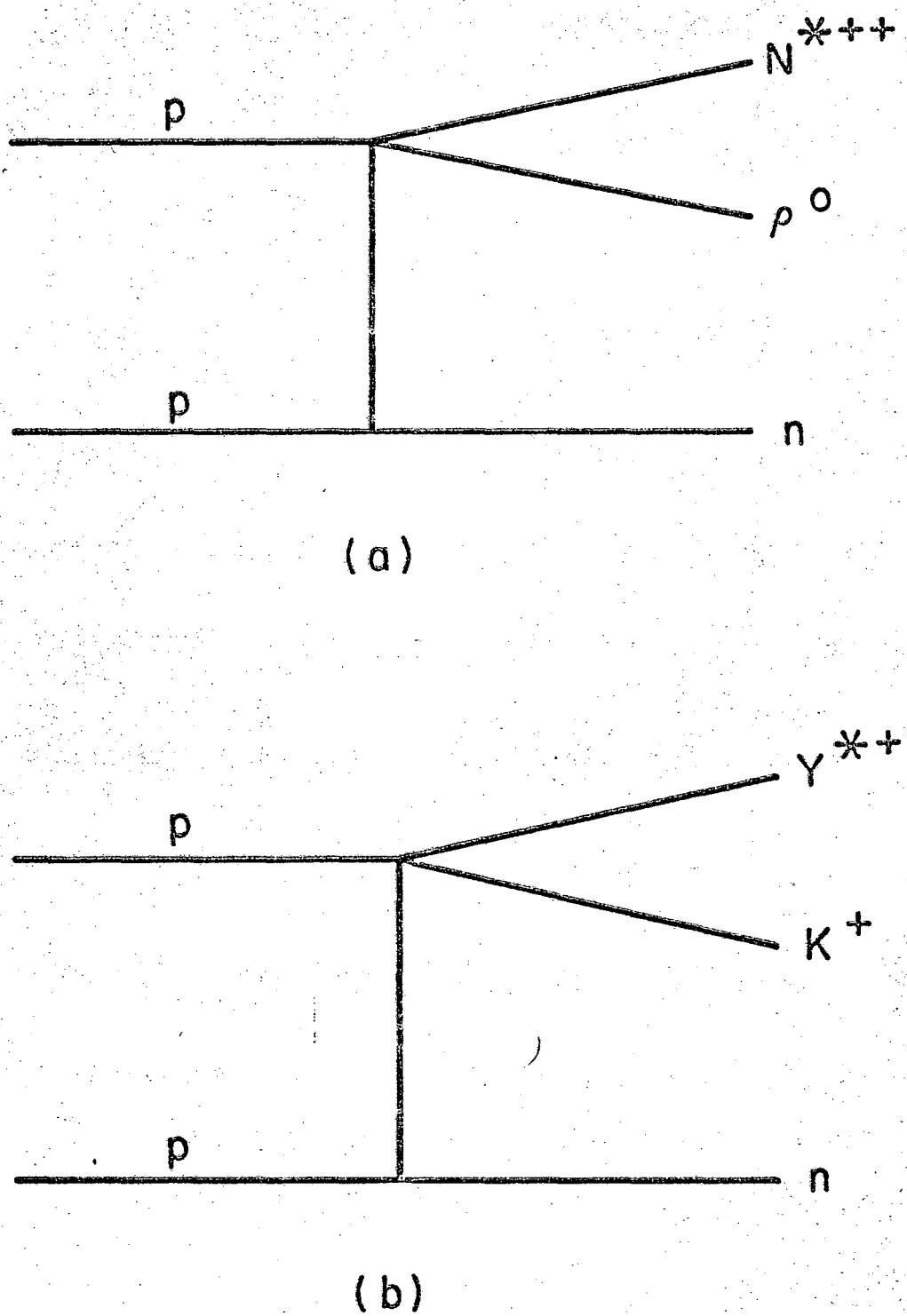

XBL6712-5938

Fig. 9

This report was prepared as an account of Government sponsored work. Neither the United States, nor the Commission, nor any person acting on behalf of the Commission:

A. Makes any warranty or representation, expressed or implied, with respect to the accuracy, completeness, or usefulness of the information contained in this report, or that the use of any information, apparatus, method, or process disclosed in this report may not infringe privately owned rights; or

B. Assumes any liabilities with respect to the use of, or for damages resulting from the use of any information, apparatus, method, or process disclosed in this report.

As used in the above, "person acting on behalf of the Commission" includes any employee or contractor of the Commission, or employee of such contractor, to the extent that such employee or contractor of the Commission, or employee of such contractor prepares,. disseminates, or provides access to, any information pursuant to his employment or contract with the Commission, or his employment with such contractor.